





Article

Prediction of Bearing Capacity of the Square Concrete-Filled Steel Tube Columns: An Application of Metaheuristic-Based Neural Network Models

Payam Sarir ^{1,2}, Danial Jahed Armaghani ³ , Huanjun Jiang ^{1,2,*}, Mohanad Muayad Sabri Sabri ^{4,*} , Biao He ⁵ 
and Dmitrii Vladimirovich Ulrikh ³ 

- ¹ College of Civil Engineering, Tongji University, Shanghai 200092, China; payamsarir@tongji.edu.cn
² State Key Laboratory of Disaster Reduction in Civil Engineering, Tongji University, Shanghai 200092, China
³ Department of Urban Planning, Engineering Networks and Systems, Institute of Architecture and Construction, South Ural State University, 76 Lenin Prospect, 454080 Chelyabinsk, Russia; danialarmaghani@susu.ru (D.J.A.); ulrikhdv@susu.ru (D.V.U.)
⁴ Peter the Great St. Petersburg Polytechnic University, 195251 St. Petersburg, Russia
⁵ Department of Civil Engineering, Faculty of Engineering, Universiti Malaya, Kuala Lumpur 50603, Malaysia; s2005282@siswa.um.edu.my
* Correspondence: jhj73@tongji.edu.cn (H.J.); mohanad.m.sabri@gmail.com (M.M.S.S.)

Abstract: During design and construction of buildings, the employed materials can substantially impact the structures' performance. In composite columns, the properties and performance of concrete and steel have a significant influence on the behavior of structure under various loading conditions. In this study, two metaheuristic algorithms, particle swarm optimization (PSO) and competitive imperialism algorithm (ICA), were combined with the artificial neural network (ANN) model to predict the bearing capacity of the square concrete-filled steel tube (SCFST) columns. To achieve this objective and investigate the performance of optimization algorithms on the ANN, one of the most extensive datasets of pure SCFST columns (with 149 data samples) was used in the modeling process. In-depth and detailed predictive modeling of metaheuristic-based models was conducted through several parametric investigations, and the optimum factors were designed. Furthermore, the capability of these hybrid models was assessed using robust statistical matrices. The results indicated that PSO is stronger than ICA in finding optimum weights and biases of ANN in predicting the bearing capacity of the SCFST columns. Therefore, each column and its bearing capacity can be well-predicted using the developed metaheuristic-based ANN model.

Keywords: structural performance; square concrete-filled steel tube columns; metaheuristic-based ANN models; predictive models



Citation: Sarir, P.; Armaghani, D.J.; Jiang, H.; Sabri, M.M.S.; He, B.; Ulrikh, D.V. Prediction of Bearing Capacity of the Square Concrete-Filled Steel Tube Columns: An Application of Metaheuristic-Based Neural Network Models. *Materials* **2022**, *15*, 3309. <https://doi.org/10.3390/ma15093309>

Academic Editor: Alessandro P. Fantilli

Received: 7 March 2022

Accepted: 29 April 2022

Published: 5 May 2022

Publisher's Note: MDPI stays neutral with regard to jurisdictional claims in published maps and institutional affiliations.



Copyright: © 2022 by the authors. Licensee MDPI, Basel, Switzerland. This article is an open access article distributed under the terms and conditions of the Creative Commons Attribution (CC BY) license (<https://creativecommons.org/licenses/by/4.0/>).

1. Introduction

Among the concrete-filled steel tube (CFST) columns, the circular CFST (CCFST) and the square CFST (SCFST) columns have a more comprehensive range of applications and are used more often than the other types in construction as these shapes are more suitable for the concrete confinement. However, the confining action could be less efficient in SCFST column due to its angles [1,2]. Nevertheless, in current global practices, SCFST columns are also applied in the main lateral resistance systems of unbraced and braced building structures, and they also might be used for retrofitting purposes in seismic prone zones. In addition to CFST columns, this type of square infilled tube can be used as beams, caissons, and piers for deep foundations [3,4].

Some research states that concrete confinement is not efficient enough in square concrete-filled steel tube columns (SCFST) because of rigidity loss in these types of columns. In fact, in these SCFST columns, only the concrete around the center and corners of the

column is restrained effectively [5]. However, various infilled concrete may behave differently to normal concrete (NC). It is of great importance that material properties can effectively influence the bonding strength between the two materials, steel and concrete [6]. In addition, the concrete's confining degree could be enhanced by decreasing the width to thickness (w/t) ratio, while a higher value of it can cause concrete crushing as well as extra local buckling [7,8].

Several experimental and computational research were evaluated the structural performance of square concrete-filled steel tube (SCFST) columns subjected to different loading conditions or various structural parameters [8–11]. Many factors, such as the section's size, length to width ratio, and wall thickness, were also evaluated by researchers and many design equations and formulas were generated or modified. However, the most significant factors influencing the structural behavior of the SCFST columns are the width/thickness ratio, concrete compressive strength, yield strength of the steel tube, and wall thickness [11–13]. Han et al. [14] investigated the behavior of the SCFST columns subjected to axial compression with a local compression area of 1.44 and 16 using experimental and numerical analysis. In total, 15 samples of SCFST columns were cast and tested in the laboratory, and they were also simulated using finite element analysis. Another study was performed by Skalomenos et al. [15] to analyze the nonlinear response of square CFSTs subjected to constant axial load. They performed a parametric study using finite element analysis to assess the expressions. The results provided the essential parameters, considering three hysteretic models, including strength and stiffness degradation. Numbers of studies were performed laboratory test for the composite columns and compared the results with the design codes in this regard such as EN 1994-1-1:2004, and GB 50936-2014. For instance, Zhang et al. [16] tested 24 composite stub columns under axial loading and compared the results with both earlier mentioned standards. In another study [17], the researchers presented a study to evaluate the grip mechanisms in infilled tube with conventional and lightweight concrete. For this purpose, they referred to different standards of AISC 360-10 and EN 1994-1-1 for the fixed value of the bond strength.

In addition to the experimental and numerical studies using finite element method (FEM), computational studies using artificial intelligence (AI) and machine learning (ML) techniques have been widely conducted in recent years. Several studies have applied artificial neural network (ANN), gene-expression programming (GEP), particle swarm optimization (PSO), imperial competitive algorithm (ICA), and many more for civil engineering applications [18–28]. Among them, some studies were conducted the application of ML/AI on the composite CFST columns. Jiang et al. [29] compared the results of the gene-expression programming with the finite element analysis of the circular CFST columns. Zarringol et al. [30] used ANN to predict the bearing capacity of rectangular and circular CFST columns under concentric loading conditions. Four extensive datasets were used to generate predictive models in their study. Recently, researchers developed a prediction model for the circular CFST column by using ANN, GEP, and the Adaptive Neuro-Fuzzy Inference System (ANFIS). Luat et al. [31] investigated a new methodology for predicting the bearing capacity of CCFST columns subjected to axial loading using a hybrid AI technique, which was developed based on the Bayesian additive regression tree and some optimization algorithms.

Moreover, an estimation to the compressive capacity of the CFST column was performed in another study carried out by Liao et al. [32] using fuzzy systems (FS). Their models applied firefly algorithm (FFA) and differential evolution (DE) techniques to obtain the optimum model. Another paper [33] presented an efficient ML-based framework to predict the strength of CFST columns subjected to concentric loading. The gradient tree boosting (GTB) technique was considered in their study. Their proposed framework was compared with other ML models such as tree-based models, support vector machines, and deep learning and showed more accurate results for the same purpose.

However, among all recent research for the concrete-filled steel tube (CFST) columns using AI/ML techniques, a few research considered the square concrete-filled steel tube

(SCFST) columns. Tran et al. [34] developed a study to predict the bearing capacity of the square CFST columns using the ANN technique. In their study, 300 experimental data samples were collected to be trained and tested. The trial–error method was applied to determine the optimum model in terms of the highest coefficient of determination (R^2) and the lowest mean square error (MSE). Furthermore, many codes were adopted to assess the performance of the study. The results showed that the ANN model was more accurate than the existing formula. After validating the ANN technique, several curves were generated to accurately analyze the SCFST columns' behavior under compressive loading. In another study [35], the short square CFST column was considered, and a comprehensive dataset was obtained by means of axial compression tests. In this research, SVM and PSO were combined to develop a new hybrid model called PSVM (SVM optimized by PSO) to predict the bearing capacity of SCFST columns. For validation purposes, the reliability of the novel model was verified against the experimental results. Le [36] proposed a model based on Gaussian Process Regression (GPR) to predict the axial load which the SCFST columns could withstand under compression, and reported a high level of accuracy for the proposed GPR model.

Furthermore, in another study [37], a GEP-based methodology is proposed to develop some equations to analyze the bearing capacity of the SCFST columns subjected to axial compression. For this purpose, six GEP-based equations were proposed. The results indicated that the proposed formulations excelled the current codes and correlations in terms of efficiency. A radial basis function neural network was applied to predict the bearing capacity of SCFST columns [38]. In this study, FFA and other optimization algorithms were also applied. A database of 300 experimental tests was collected from the literature to train the data. Several comparative criteria were also used to assess the accuracy of the proposed model. The outcomes revealed that the novel predictive model could provide a higher accuracy compared with the other similar techniques.

In structural engineering, it is essential to study the bearing capacity of the CFST columns, specifically, the SCFST column, since the grip between steel tube and concrete core in these sorts of columns is complicated, and the structural performance of these columns is often nonlinear as a result of this interaction. Furthermore, the experimental laboratory tests are generally expensive and time-consuming. In recent years, using artificial intelligence (AI) methods have become more popular as the AI approaches are usually faster and less complex in comparison with FEA. The accuracy of prediction in simulation by FE method is highly influenced by input elements which normally cannot be simulated thoroughly [39]. Therefore, using AI/ML methods for predicting the bearing capacity of the SCFST columns could be a suitable alternative. Due to the lack of research in terms of developing AI/ML techniques to predict the ultimate bearing capacity of the square CFST columns, this study aims to propose a novel technique using a combination of ANN and metaheuristic algorithms (i.e., PSO and ICA) for prediction of the ultimate axial load of these types of columns. The step-by-step modeling procedure is explained, and the obtained results are compared to select the best ANN-based metaheuristic model.

2. Methods

2.1. Artificial Neural Network

The artificial neural network (ANN) is a method that takes advantages of a biology-based computational model that resembles the rational reactions of a human brain. ANN is a methodology for recognizing sophisticated relationships between different variables, resulting in computational models for one or a number of outputs [40–42]. Basically, an ANN model encompasses three fundamental components named “activating function”, “patterns of connections”, and learning rules [43]. Depending on the problem that needs to be taken into account, the components are required to be introduced to train the network considering their weights [44]. In this regard, one of the ordinary neural networks is the multilayer perceptron (MLP), which consists of a layer of input variables, one or more hidden layers of neurons' processing, and a layer for output variables. All of these layers

are connected in a sequential order, and the latter layers usually include one or more neurons together with numerical operators. Essentially, a feedforward is responsible for making signals between the output and input layers through the hidden layers. In order to specify the features of input variables, the signals, initially, have to be assessed through the hidden neurons. Later on, the specified features will be transferred to the neurons in the output layers to generate a proper model [45,46].

In recent years, various learning techniques have been suggested to improve the capability of MLP. However, backpropagation (BP) was considered a more effective method based on gradient descent [47]. This technique is benefitted from interchanging the input signs between the nodes of sequential layers. In this method, the net weight of each input “ net_j ” is calculated as the following:

$$net_j = \sum_{i=1}^n x_i w_i^{-\theta} \quad (1)$$

In which n is the input’s quantity, x_i is the input’s signal, and w_i represents the weight of each node. Furthermore, the threshold of each node determines by the θ parameter. The activation functions, such as sigmoid, linear function, and step, are responsible for passing through the input variables, which is called the training step of the variables. In the next step, a comparison between the actual output and the predicted one will be made, and the discrepancy between these two can be determined [48]. Finally, the calculated errors travel back into the network to refresh the individual weights. Figure 1 indicates a numerical model for artificial neurons. During the training stage, the network behavior is assessed through proper statistical functions such as the root mean square error (RMSE) [44]. The refreshing of the weights will be continued until the system observes a decline in RMSE lower than a predefined level. The number of datasets is a significant factor in this technique, as lack of it may lead to overfitting in the training process [49].

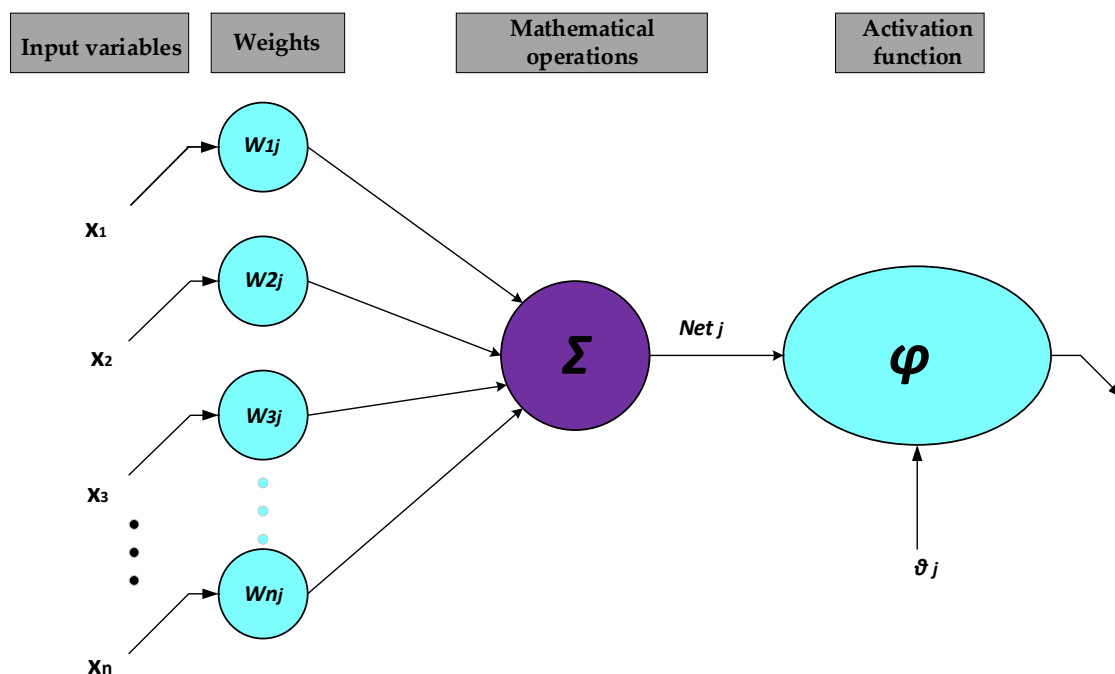


Figure 1. ANN structure.

2.2. Particle Swarm Optimization

In 1997 [50], Kennedy and Eberhart first proposed an intelligent computer-based technique for optimization, which later it is called particle swarm optimization (PSO). This methodology mimics the natural behavior of some creatures, such as birds, fish, bees, and

ants [51]. Several algorithms later followed this technique, such as the ant colony algorithm (ACO). While some similarities exist between ACO, PSO, and genetic algorithm (GA); PSO has less complexity. In fact, PSO randomly takes advantage of the actual numbers and the relationships between the swarm particles. In the PSO technique, some entities, named particles, are distributed in an area called the objective function's zone. The main concept in this algorithm is to locate the particles in their optimal conditions. The main elements in the particles' movement are deterministic components and characteristics of stochasticity. In addition, they can move towards the existing global best (p^*) and also it is the best location (x_i^*). Later on, the particle will look for a more suitable location compared with the previous one. In any time, " t ", of the specific iterations, a current best location for the n particles is available. Particles, finally, will look for the global best to end up with the algorithm. Figure 2 illustrates the movements of particles. As evident from the figure, x_i^* is the current best for the particle i , and $p^* \approx \min\{f(x_i)\}$, ($i = 1, 2, \dots, n$), is the global best.

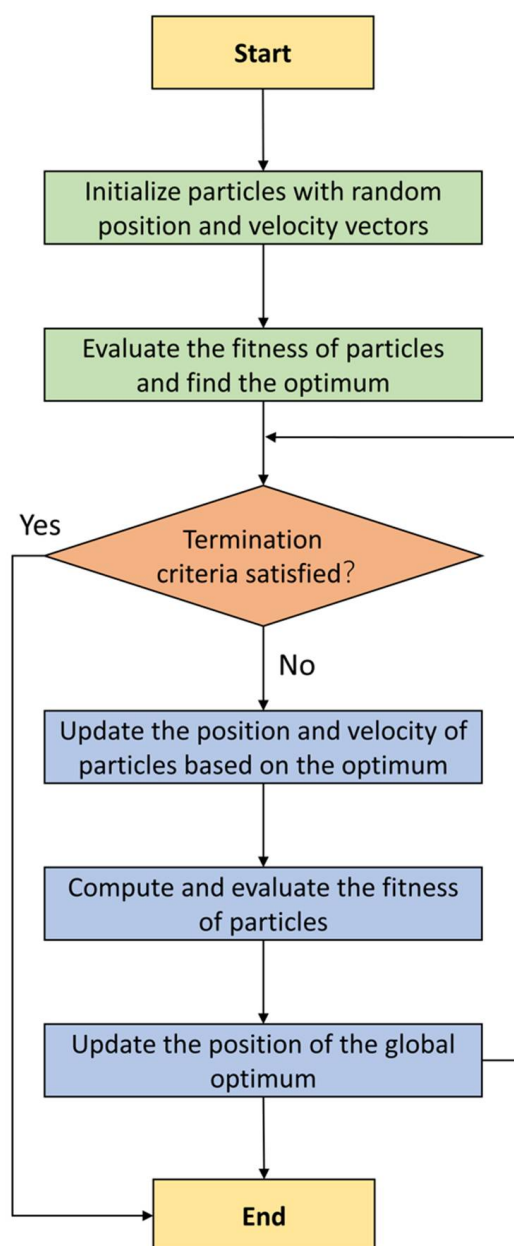


Figure 2. PSO algorithm to optimize problems.

Using Equation (2), given the fitness requirements for the swarms, the velocity of the swarms may be determined by a function that is proportional to the best location of the swarm and the most suitable position of each particle. Furthermore, Equation (3) leads to the successive suitable positions of the particles.

$$\vec{v}_{\text{new}} = \vec{v} + C_1 \times (\vec{p}_{\text{best}} - \vec{p}) + C_2 \times (\vec{g}_{\text{best}} - \vec{p}) \quad (2)$$

$$\vec{p}_{\text{new}} = \vec{p} + \vec{v}_{\text{new}} \quad (3)$$

In these equations, \vec{v}_{new} , \vec{v} , \vec{p}_{new} , and \vec{p} signify the new velocity, the current velocity, the new position, and the current position of particles. C_1 and C_2 shows predefined coefficients; \vec{p}_{best} is the best position of the particle itself, and \vec{g}_{best} represents the global best position among all particles. Poli et al. [52] stated that Equation (2) could be adjusted if a new parameter, inertia weight (w) is added to it. Inertia weight specifies the rate of the previous velocity of each particle to its velocity at current Equation (4). The flowchart of PSO algorithm is illustrated in Figure 2.

$$\vec{v}_{\text{new}} = w \cdot \vec{v} + C_1 \times (\vec{p}_{\text{best}} - \vec{p}) + C_2 \times (\vec{g}_{\text{best}} - \vec{p}) \quad (4)$$

2.3. Imperialism Competitive Algorithm

When it comes to engineering challenges, the ICA, created by Atashpaz-Gargari and Lucas [53], is one of the most effective optimization strategies. Similar to the other techniques, ICA begins its processing by making “so-called countries” as a random initial population. After making N countries (N_{country}), many of them having the lowest costs or functions, are picked up as the imperialists (N_{imp}). As a result, colonies (N_{col}) are specified as the remaining countries. Based on the power of empires, all colonies will be distributed to them [54,55]. Therefore, the more influential the imperialists (lowest RMSE), the more colonies can be absorbed. ICA comprises three leading operators, which are revolution, assimilation, and competition. While assimilation and revolution are in operation, a colony can reach a zone that is superior to that of its imperialist neighbor and seize control of the territory formerly controlled by the preceding imperialist.

However, since it is a competitive scenario, each empire has a chance to dominate at least one colony of the weakest empire, depending on the strength of the empire in question. Suppose the most powerful empire is still undefeated after a certain number of iterations or decades. In that case, the method will be repeated until a specified termination condition is satisfied, such as an acceptable RMSE, a maximum number of iterations or decades, etc. Note that the number of decades (N_{decade}) in ICA is potentially quite comparable to the number of iterations in several other algorithms, which is worth noting [56,57]. The flowchart of ICA is shown in Figure 3.

2.4. Metaheuristic-Based ANN Models

The problem in using ANN in prediction case studies is that it will receive different results with various performance levels. It is because of the basic shortcomings of ANN, which are slow learning rate and getting trapped in local minima [58,59]. In these conditions, the possible solutions may refer to optimizing weights and biases of ANN and therefore getting more similar results by means of ANN. This optimization process can be performed by metaheuristic algorithms such as PSO and ICA. These algorithms and their effective parameters should be designed to obtain the best optimization outcome. For example, the number of countries and swarms should be designed based on a series of available range introduced in the literature. Of course, the results of hybrid models cannot differ significantly in terms of specific influential parameters. The flowcharts of hybrid models used in this study to solve the bearing capacity of the SCFST columns are presented

in Figures 4 and 5. As it can be seen from these figures, a number of populations (i.e., particles or countries) together with the other effective parameters of the optimization algorithms are selected and the hybrid system is trained. Then, the error indicators of the hybrid system should be measured based on the optimum weights and biases of ANN itself. Because the goal is to achieve the lowest system error possible, different values of optimization parameters can result in different system errors for the entire system. Therefore, each effective parameter should be designed using a trial-and-error system. It is worth mentioning that the base model should be designed using ANN itself. These hybrid models been applied to get more stable results in different areas of civil engineering [60,61].

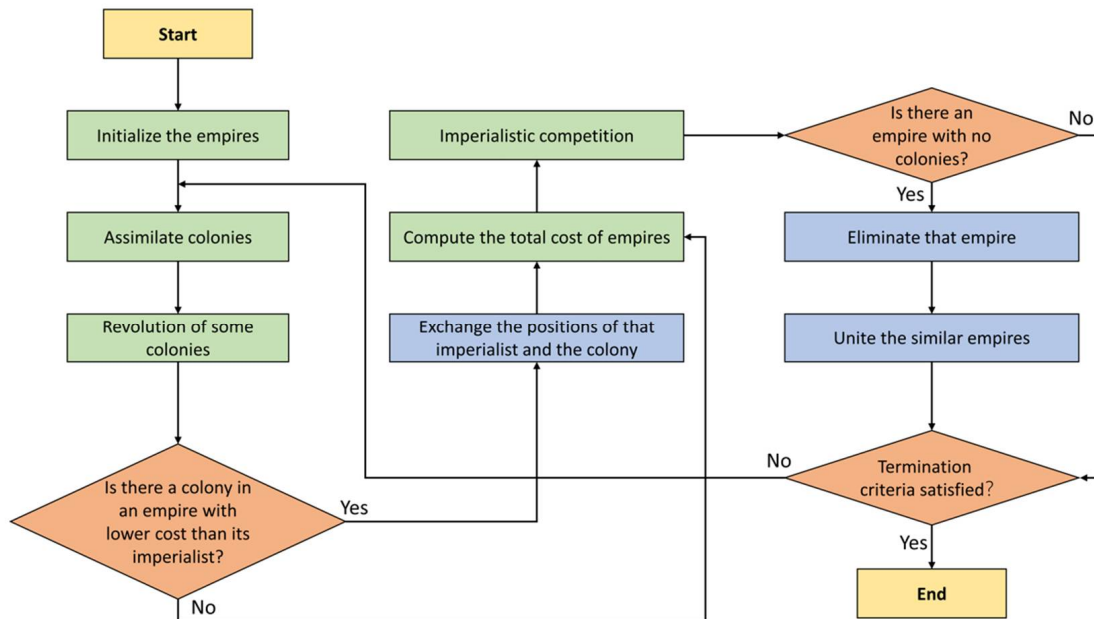


Figure 3. ICA algorithm to optimize problems.

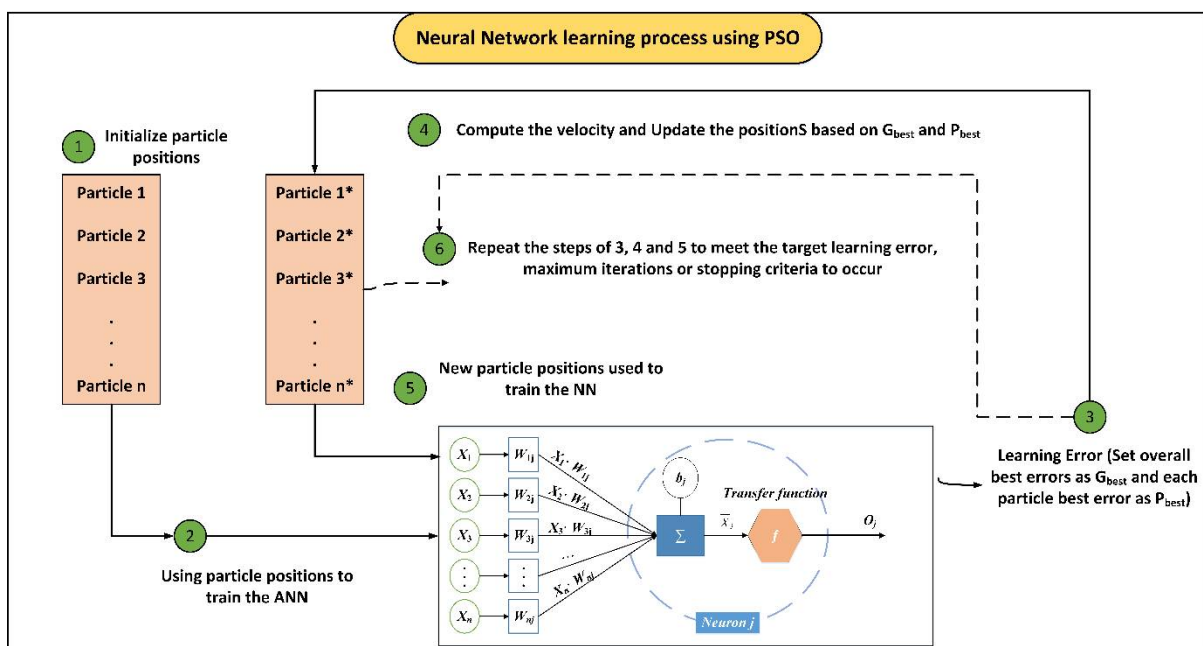


Figure 4. PSO-ANN algorithm.

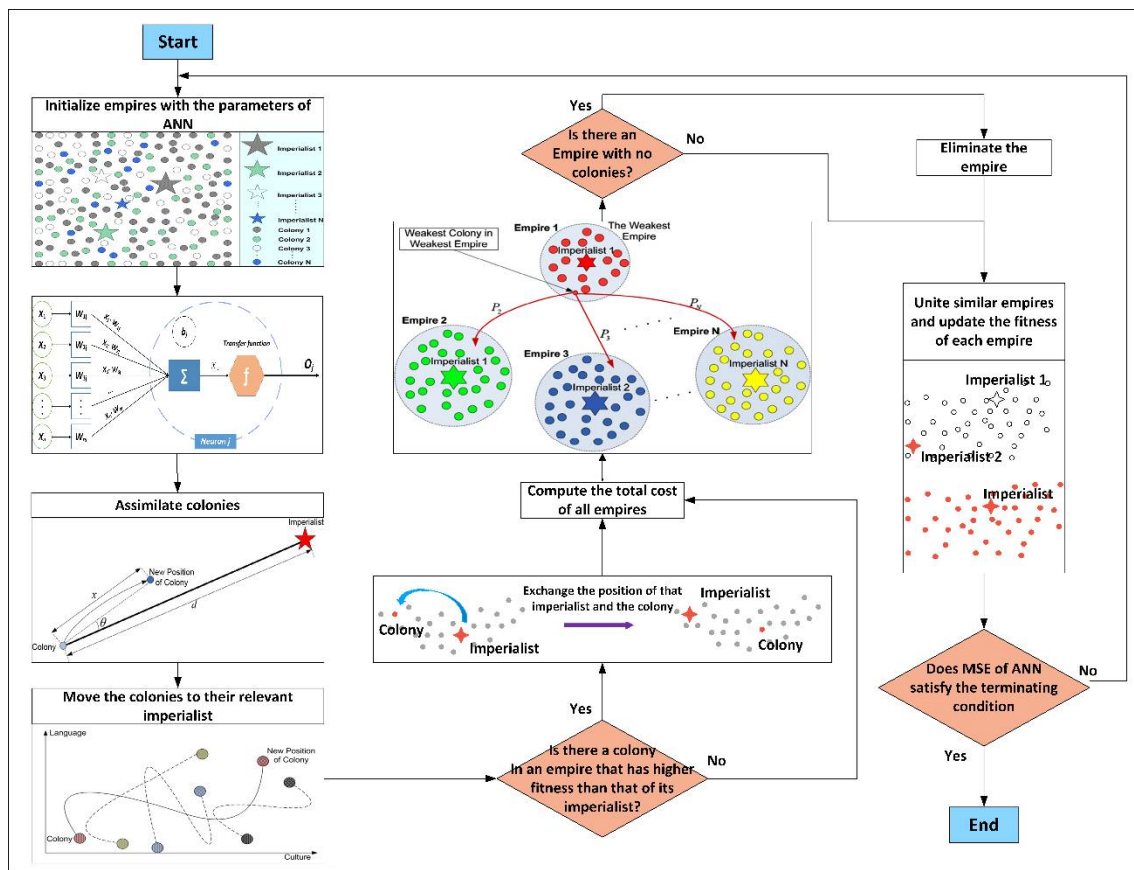


Figure 5. ICA-ANN algorithm.

3. Data Source and Input Parameters

3.1. Background

For many years, types and shapes of columns have been developed from typical reinforced concrete columns and steel columns into steel-reinforced concrete columns and various types of composite columns such as CFST columns, encased columns, and also concrete columns reinforced with concrete-filled steel tubes. Improvements and revolutions in CFST have rapidly grown during the past decades until now. Different technical journals on this topic led to the establishment of the Architectural Institute of Japan (AIJ) and a standard for circular steel and concrete, which is known as a composite structure, released in 1967. Japan and China conducted many investigations to lay the foundation for CFST later on. Then, in 1993, a study plan on composite and hybrid structures, the fifth stage of the US-Japan collaboration research program, and another study on CFST column systems were considered in the study, and the findings achieved from this investigation made the current design suggestions for the CFST column system.

CFST columns demonstrate more fire resistance and strength property levels than bare steel columns [62]. In addition, the filled concrete has a significant role in the structural behavior of these types of columns. High-performance concrete has superior characteristics compared to NC, for example, improved ductility, strength, and self-consolidating features. Using high-performance concrete, including lightweight concrete (LWC) and engineering cementitious concrete (ECC), could improve the ductility and strength of the concrete-filled tube composite columns. Several studies investigated self-consolidated concrete (SCC) and the NC-filled tube columns [63]. However, the current study attempts to collect comprehensive data from the literature consisting of square CFST columns with various concrete compressive strengths purely under axial compression. This limitation of datasets is due to achieving better results through prediction using ML/AI techniques. Figure 6 indicates a schematic of using ML/AI techniques for the square CFST columns.

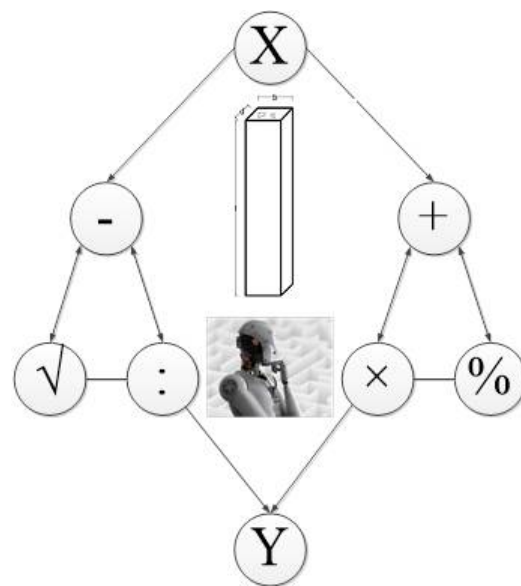


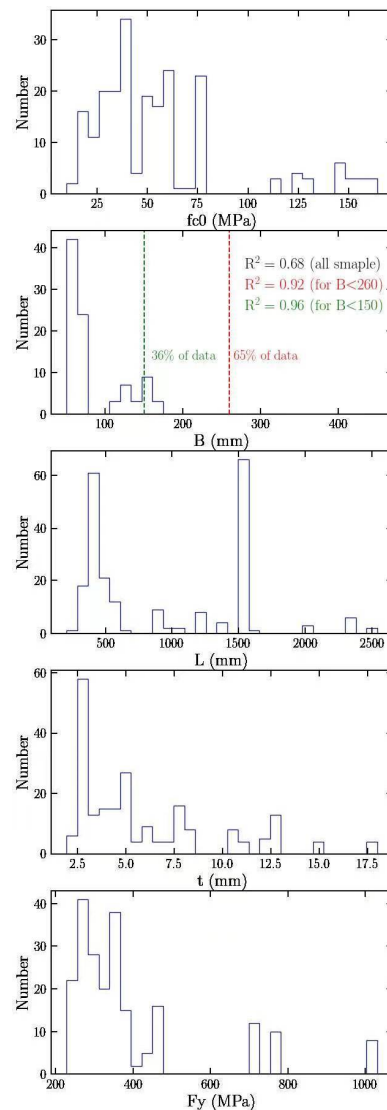
Figure 6. The schematic of using AI techniques for the SCFST columns.

3.2. Data Source

This study tries to collect extensive datasets from the literature. More than a hundred articles were studied, and among them, twenty-three articles were chosen to include their results in the dataset of this study because some of the studied articles were comprised of SCFST columns under different loading conditions or some of them with additional reinforcements inside the column, which could highly impact our result of the ultimate bearing capacity. At first, 217 data points were achieved from the articles that were taken into consideration [13,14,61,63–76]. Several essential parameters can affect analysis and results based on the previous experimental tests and experience [69,70,76,77] and some of the former data analysis for the CFST columns [26,31,35,78–80]. They are concrete compressive strength (f_c), the width or diameter (B/D) of the columns, the length of column (L), the thickness of the columns (t), the yield strength (f_y) of the steel tube, the slenderness ratio (L/D , B), and the diameter/width to thickness ratio (D , B/t). However, the most critical factors for the SCFST columns which impact the ultimate bearing capacity (P_{exp}) were considered as five factors: concrete compressive strength (f_c), the column's width (B), the column's length (L), the column's thickness (t), and the yield strength (f_y) of the steel tube. The minimum, maximum, average, and standard deviation values of the first patch of the collected data are shown in Table 1. The initial raw data were first analyzed considering empirical analysis and try and error. For this purpose, by taking all input parameters into consideration, the distribution of each was plotted, and later, it was considered which parameter had the most impact on the output, which was the bearing capacity, in this study. Then, considering the parameters with the dispersed data and eliminating those, it was found that which parameters had a higher impact on the R^2 . Therefore, after the preliminary analysis, it was revealed that the first patch of the collected data has a wide range of tolerance, which can cause less accuracy from the machine learning techniques. It was more critical for the wide range of the width of the columns. As shown in Figure 7, when all data were considered, the initial R^2 was 0.68, while after the column's width filtration to less than 260 mm and 150 mm, the R^2 value was increased to 0.92 and 0.96, respectively, which is highly improved. It is worthy of mention that the R^2 value is one of the significant factors in ML/AI to be considered for training and testing stages. The closer the value of R^2 to 1, the better results can be achieved from training and testing sessions.

Table 1. Statistical distribution of data.

Parameter	Min	Max	Average	Std. Dev
f_c (MPa)	10	164	55.66	35.25
B (mm)	50.8	450	208.55	106.80
L (mm)	210	2540	937.10	575.45
T (mm)	1.94	18	5.90	3.70
f_y (MPa)	229	1030.60	394.60	184.25
P_{exp} (kN)	329	8912	2139	1802.60

**Figure 7.** Statistical distribution of the first patch of data.

Therefore, it was decided to sort the data based on the preliminary results. The updated dataset led to 149 pure data points, where the range of the data was closer to each other to achieve more accurate results. Finally, the following ranges were considered in this study: 20–130.8 MPa for the concrete compressive strength (f_c), 80–450 mm for the outer width (B) of the column, 295–2340 mm for the length of the column (L), 1.94–11.25 mm for the thickness of the steel cover (t), 231–1030.6 MPa for the tensile yield stress of the steel column, and 490–3922 kN for the bearing capacities of CFST columns. The updated statistical distribution of the values is indicated in Table 2.

Table 2. Statistical distribution of data used in the modeling.

Parameter	Min	Max	Average	Std. Dev
f_c (MPa)	20	130.8	47.70	24
B (mm)	80	450	198.50	94.90
L (mm)	295	2340	927.75	530.10
T (mm)	1.94	11.25	5.10	2.40
f_y (MPa)	231	1030.60	377.20	184.60
P_{exp} (kN)	490	3922	1588	843.70

In addition, in order to show the correlation between independent variables and dependent variables, the correlation matrix was used. The correlation matrix is a matrix that can be used when several inputs can generate R^2 (or else) with their pairs. However, it is worth mentioning that only the linear correlations between two variables can be evaluated with this approach. Therefore, it may not be capable of being used for nonlinear relationships. Figure 8 illustrates the correlations between the variables with their adjusted R^2 values. In addition, the distributions for each parameter are presented in Figure 8. In general, the relations between variables are not that high and significant. The highest correlation between input parameters is related to the relationship of T (mm) and B (mm) with $Adj R^2 = 0.592$ followed by the relationship of L (mm) and B (mm) with $Adj R^2 = 0.531$. In terms of input–output relationships, f_y received the highest $Adj R^2$ (0.518) for predicting P_{exp} followed by f_c with $Adj R^2 = 0.195$. It seems that proposing a multi-inputs model with a high level of accuracy is of importance based on these simple regression analyses.

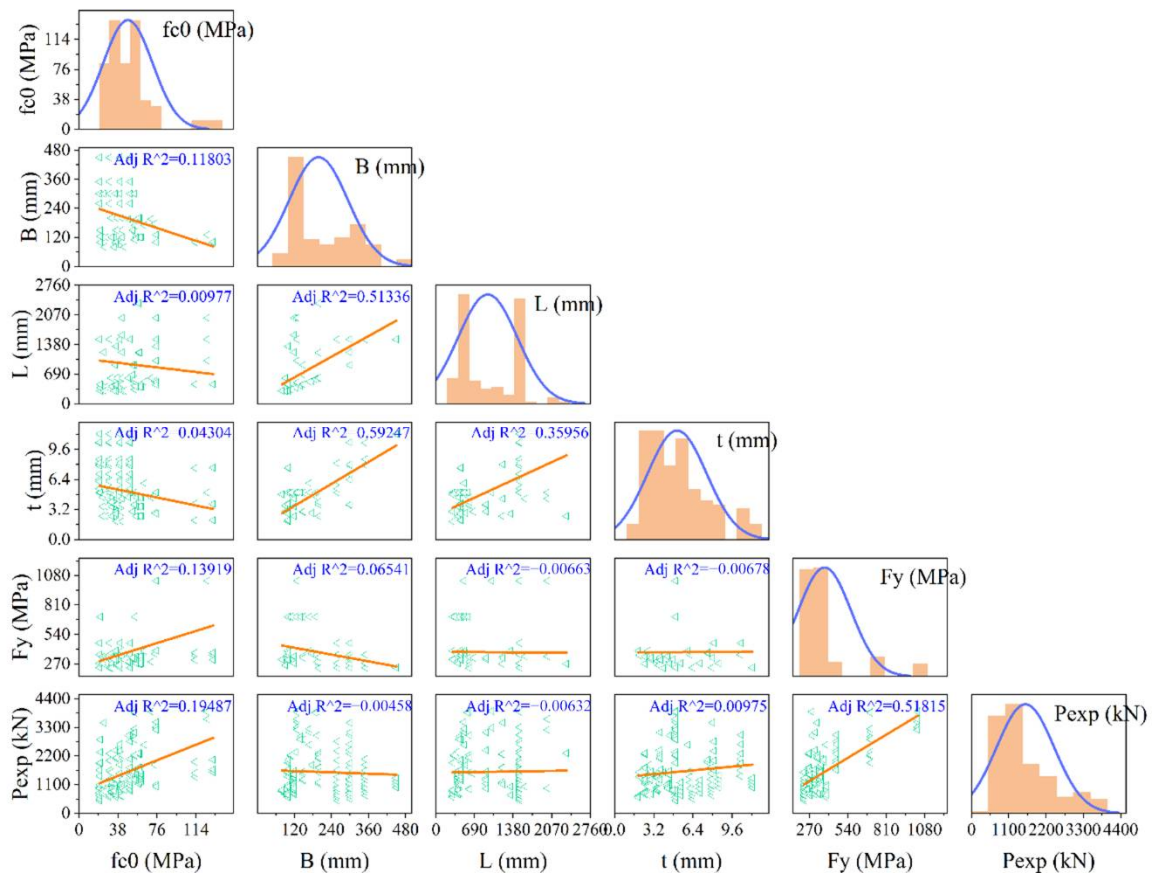


Figure 8. Correlation matrix for the input and output variables.

4. CFST Prediction

The most important parameters of the ANN system should be determined before beginning the modeling steps. However, the data samples must be normalized before this can be carried out. It was recommended by Liou et al. [81] that a specific equation can be used to normalize datasets at the modeling outset in order to simplify the process:

$$X_{\text{normalize}} = (X - X_{\text{minimum}}) / (X_{\text{maximum}} - X_{\text{minimum}})$$

where $X_{\text{normalize}}$, X_{minimum} , and X_{maximum} are the normalized data sample, the minimum of each data sample, and the maximum of each data sample, respectively.

ANN models with just one hidden layer [30,34,44] or multiple hidden layers [82,83] were presented by a number of researchers to solve various problems [45,46]. To anticipate the bearing capacity of the SCFST columns, we analyzed data from the first three layers of our data. The findings of this parametric investigation (PI) revealed that when they are compared to other implemented numbers, one hidden layer provided more accurate prediction performance than the others. ANN performance is also affected by the number of neurons in the network, which should be calculated using a different PI analysis. Preliminary research revealed that the hidden neuron values in the range of 1–11 should be considered and employed in the modeling of this section, where their root mean square error (RMSE) values were examined. As a result of these PIs, it was discovered that the hidden neuron number 9 produces bearing capacity values that are more similar to the measured values. As a result, this value was chosen as the optimal ANN model. Based on the findings from these PIs, a model with five input variables, nine hidden neurons, and one output neuron is introduced as the best ANN model, and all further hybrid modellings in this study are carried out using this model as a reference. The training and testing datasets for this investigation were selected at random from a pool of data samples representing 80% and 20% of the total number of data samples, respectively. It means that the numbers of 30 and 119 were considered for training and testing purposes of this study.

A major step in the PSO-ANN modeling process is to choose an appropriate particle size and number of iterations simultaneously during the initial stage. Through another PI, the swarm size was specified to be in the range of 50 to 500 (50, 100, 150, 200, 250, 300, 350, 400, 450, and 500). On the other hand, it was decided to set the maximum number of iterations as 500. Thus, 10 PSO-ANN prediction models were developed to forecast the bearing capacity of the SCFST columns, using the RMSE results as shown in Figure 9. As evident from the figure, the RMSE values for all of the models were significantly lowered at the beginning of the iterations. After that, the modification of the values was minimized progressively until attaining a constant value. In this manner, the situation in which the swarm size was set at 150 was the one in which the lowest error was attained. Furthermore, it can be noted that the RMSE reached a constant value after 350 rounds. As a result, to anticipate the bearing capacity of the SCFST columns for the purposes of the modeling presented in this work, the swarm size and the number of iterations used in the current article were set at 150 and 350, respectively. It is worth noting that these models were built using $C_1 = C_2 = 2$ and $w = 0.25$.

On to the second step, the C_1 and C_2 parameters were calculated. A PI was built similarly to the previous phases, using a variety of C_1 and C_2 values to examine which ones were the most appropriate for our model. In order to do this, the PSO-ANN models were built using the following parameters: ($C_1 = C_2 = 2.5$), ($C_1 = C_2 = 2$), ($C_1 = C_2 = 1.75$), ($C_1 = C_2 = 1.5$), ($C_1 = 2$ and $C_2 = 1.5$), and ($C_1 = 1.5$ and $C_2 = 2$). As a factor for assessing the models' prediction performance, R^2 was considered. Figure 10 indicates the results in this regard. The best model was obtained with $C_1 = C_2 = 2$ as its training and testing R^2 values are the highest among all six models shown in Figure 10. Consequently, both C_1 and C_2 were set to 2 and applied to the last modeling step, which was responsible for computing the "w" value.

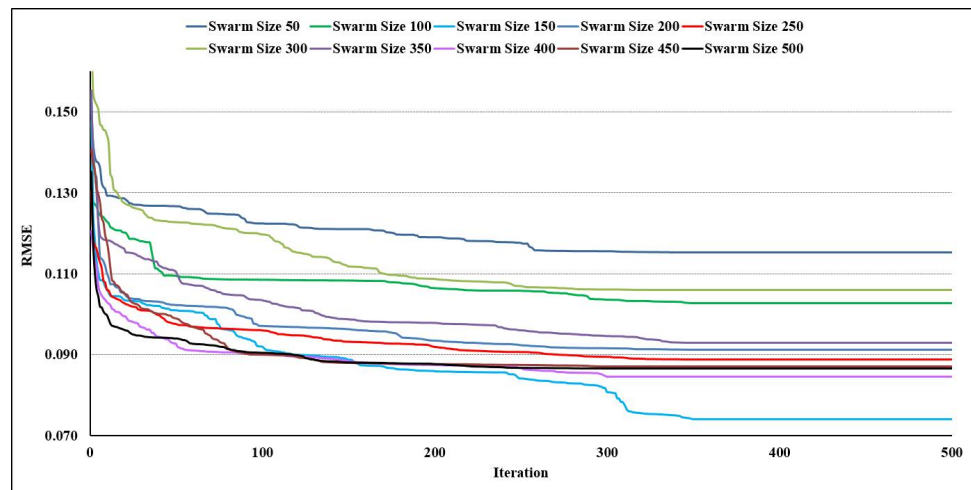


Figure 9. Ten PSO-ANN models and their RMSE results.



Figure 10. C_1 and C_2 results in PSO-ANN models.

The accuracy level of the PSO-ANN models is also affected by the “w” value, which can significantly influence these models [84]. As a result, in the four PSO-ANN models shown in Figure 11, the “w” value was adjusted to 0.25, 0.5, 0.75, and 1. Once again, R^2 was selected as the performance criterion in this PI. As evident from the figure, the PSO-ANN model with $w = 0.25$, presented the best ability to fit and predict the bearing capacity of the SCFST columns. Therefore, as a summary for the best PSO-ANN model, the values of 150, 350, 2, 2, and 0.25 were obtained for swarm size, iteration number, C_1 , C_2 , and w , respectively. This model will be further discussed in the next section.

The procedures used by the ICA-ANN approach to model the bearing capacity of the SCFST columns are discussed herein. As previously stated, three factors, namely, N_{decade} , N_{imp} , and $N_{country}$ have a substantial impact on the performance capability of the ICA-ANN. As a result, designing these parameters and acquiring the optimal parameters values using various PIs is necessary to accomplish the desired results. The first PI was carried out to pick N_{decade} and $N_{country}$ at the same time. Towards to the end, the first PI was structured similarly to the preceding section and based on a variety of previously conducted research [14,50]. In order to have a fair comparison with the PSO-ANN model, the authors decided to select and use the same values of swarm for $N_{country}$. As shown in Figure 12, the findings obtained from different $N_{country}$ are dependent on N_{decade} that have passed and they were compared in terms of predicting the bearing capacity of the SCFST

columns. As the figure simply illustrates, the majority of the countries had final RMSE values in the range of 0.11 to 0.14. When $N_{country}$ was limited to 450, the RMSE was reduced to its bare minimum. A further finding is that when N_{decade} was set around 250 (almost for all $N_{country}$), no further drop in RMSE was found. Therefore, the mentioned numbers were selected for these significant parameters of ICA ($N_{country}$ and N_{decade}).

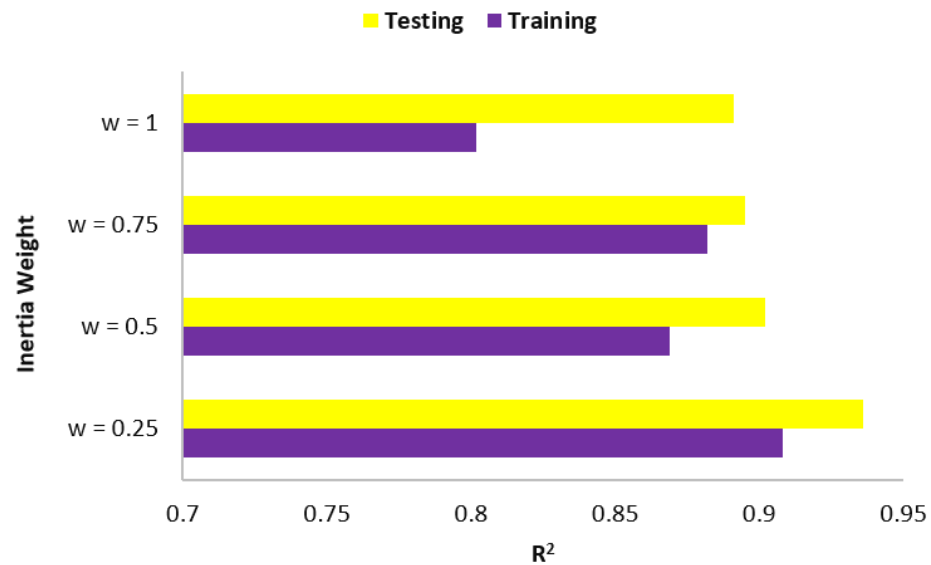


Figure 11. Results of w in PSO-ANN models.

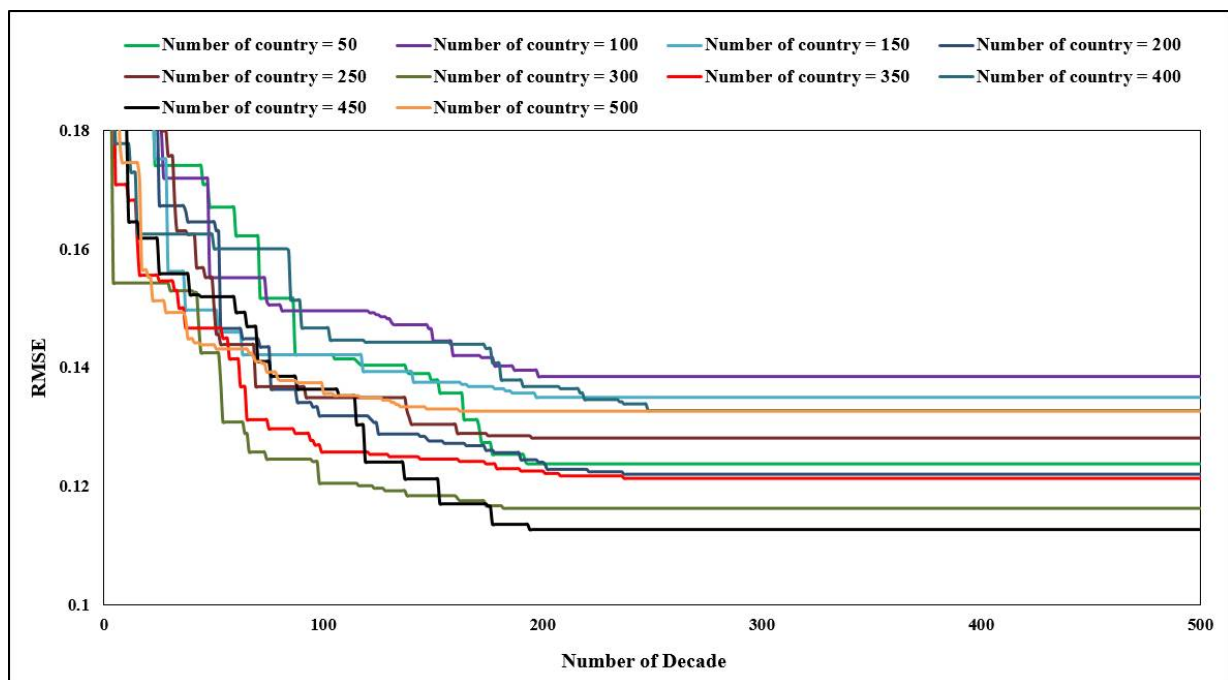


Figure 12. Ten ICA-ANN models and their RMSE results.

It is now necessary to run another PI to identify the appropriate value for the amount N_{imp} . According to previous studies, this was accomplished by varying N_{imp} from 5 to 10 [19,85]. The results achieved by this PI based on R^2 , are shown in Figure 13. Although the obtained results are close to each other and they are in a certain range, $N_{imp} = 5$ received more accurate prediction values for the bearing capacity of the SCFST columns. The R^2 values are 0.855 and 0.873 for training and testing phases, respectively. Therefore, they

were considered as the best ICA-ANN model since there are no more parameters to design. This model and its findings are discussed with further detail in the next section.



Figure 13. Results of N_{imp} in ICA-ANN models.

5. Results and Discussion

The findings of the metaheuristic-based ANN techniques in predicting the bearing capacity of the SCFST columns are addressed in this section. As previously stated, R^2 and RMSE were used to evaluate models during their building. Another statistical index, namely variance account for (VAF), was considered and calculated for the best metaheuristic-based models. The statistical indices used in this study were widely applied in other predictive studies [21,86–93]. It is important to note that this study aims to compare the ability and power of two metaheuristic-based ANN models in predicting the bearing capacity of the SCFST columns. According to previous studies [5,7,16,94], these metaheuristic-based ANN models can achieve higher performance capacities and closer predictive values than the ANN model itself. Table 3 presents the results of statistical indices for training, testing, and all datasets of PSO-ANN and ICA-ANN models in estimating the bearing capacity of the SCFST columns. The obtained results clearly showed that PSO is the most successful model in finding the optimum values for weights and biases of ANN. This model has better performance in terms of all R^2 , VAF, and RMSE statistical indices.

Table 3. Results of training, testing, and all data samples in predicting the bearing capacity of the SCFST columns.

Metaheuristic-Based ANN Model	Training		
	VAF (%)	R^2	RMSE
ICA-ANN	84.873	0.855	0.097
PSO-ANN	90.549	0.908	0.077
Model	Testing		
ICA-ANN	87.264	0.873	0.085
PSO-ANN	93.497	0.936	0.059
Model	Training + Testing		
ICA-ANN	85.296	0.857	0.094
PSO-ANN	91.125	0.913	0.074

To better understand these metaheuristic-based ANN models and their capacity for forecasting the bearing capacity of the SCFST columns, the measured and predicted values (i.e., normalized) for PSO-ANN and ICA-ANN models are displayed in Figures 14 and 15, respectively. The PSO-ANN model could provide a stronger correlation between the measured and estimated bearing capacities of the SCFST columns. This model has a strong capability during the training and testing stages and, of course, for all data samples. With the anticipated and observed bearing capacities of the SCFST columns shown in Figures 14 and 15, it is evident that PSO has significant potential for optimizing the weights and biases of ANN. If the weights and biases of the ANN were adequately optimized in the first place, the PSO-ANN model's performance capabilities could be far greater than those of the ICA-ANN model. When a system error is considered, it is clear that the PSO method outperforms the ICA approach by a significant margin. Based on the above description, it is reasonable to develop the PSO-ANN model, which can get RMSE values of (0.077 and 0.059) and VAF values of (90.549% and 93.497%) for the training and testing datasets, respectively. The generated PSO-ANN technique was found to be more powerful and adaptable than the developed ICA-ANN technique in terms of solving the described issue linked to the bearing capacity of the SCFST columns.

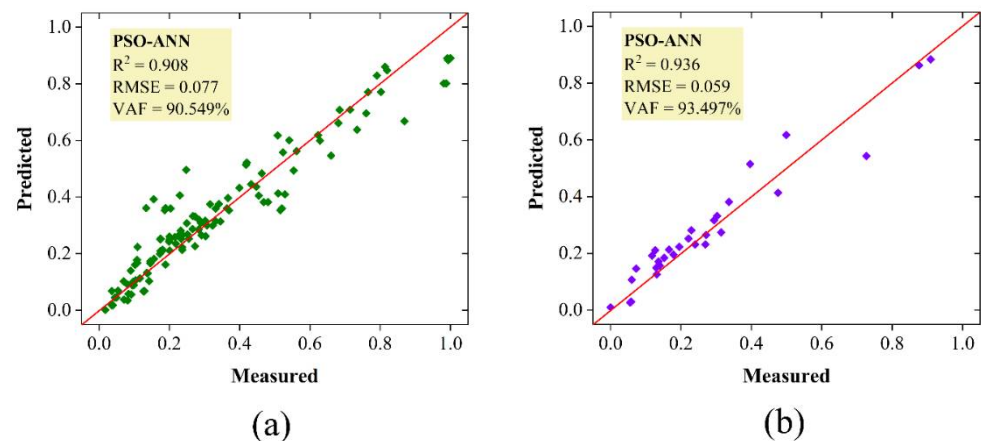


Figure 14. The results bearing capacity of the SCFST columns by PSO-ANN; (a) training, (b) testing.

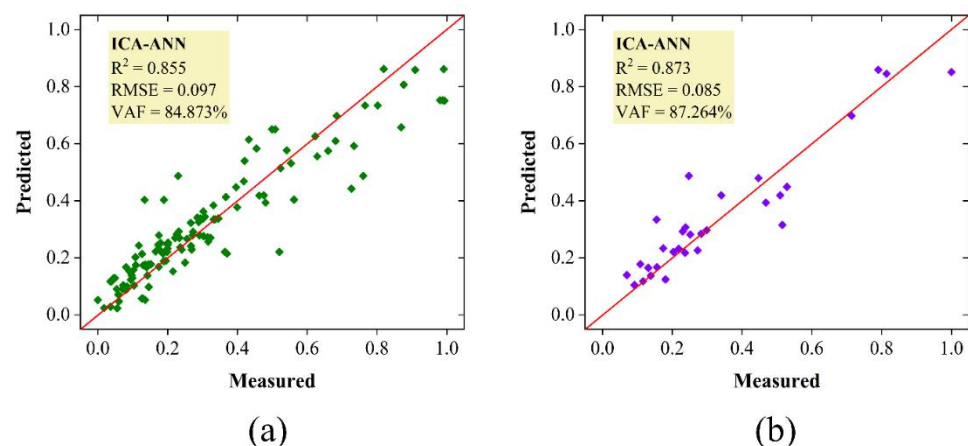


Figure 15. The results bearing capacity of the SCFST columns by ICA-ANN; (a) training, (b) testing.

In addition, in order to show the capability of the proposed models better, the results were compared with those obtained from the standards Euro Code 4 (EC4) and ACI Code [7,95]. Table 4 shows 30 data samples (which were randomly taken from the whole data) and their experiment bearing capacity results. In addition, predicted bearing capacity results by the PSO-ANN, ICA-ANN, EC4, and ACI are shown in Table 4. As clearly

indicated, the measured results by the two metaheuristic-based ANN models are much closer than the obtained results by the standard equations. It is worth noting that for the predicted results by PSO-ANN from 30 samples, 23 data have a difference of equal or less than 10%, while for the rest of the data, the discrepancy is still less than 15%. For the ICA-ANN, the difference of the predicted bearing capacities is less than 20%. For some of the datasets, for example, datasets No. 6, 8, 9, 11, 12, 23, 26, and 31, the difference between the value obtained by the PSO-ANN method and ICA-ANN method is very small. However, the bearing capacities obtained by standards formula have a difference of 11% to 56%, which in most cases, this discrepancy is more than 20% for the models. Therefore, this indicates that the proposed metaheuristic-based models are well organized to predict the bearing capacity of the SCFST columns of the same type.

Table 4. Comparison of the experimental results with predicted ones.

No.	P_{Exp} (kN)	$P_{PSO-ANN}$ (kN)	$P_{ICA-ANN}$ (kN)	P_{EC4} (kN)	P_{ACI} (kN)
1	2275	2230	2163	2785	2520
2	1760	1625	1577	2751	2418
3	2985	2823	2738	2666	2415
4	3900	3723	3612	3441	3073
5	768	845	680	660	656
6	1426	1403	1361	1176	1059
7	1302	1445	1464	1136	1025
8	990	1007	1018	923	858
9	965	854	829	826	775
10	890	895	868	783	738
11	1530	1552	1505	1240	1127
12	1367	1355	1314	1202	1094
13	1088	971	942	940	932
14	1176	1269	1290	994	930
15	1160	1042	1011	900	851
16	1090	923	896	858	815
17	1630	1841	1890	1299	1190
18	1484	1592	1602	1262	1159
19	934	849	824	601	560
20	1934	2145	2242	1502	1477
21	2828	2995	3109	2445	2383
22	2238	2279	2300	2517	2284
23	956	1029	1070	1205	1127
24	3302.4	3450	3556	3666	3502
25	3203.8	3256	3280	3666	3502
26	3611.6	3523	3418	4383	4112
27	3474	3240	3120	4988	4695
28	840	732	702	572	553
29	860	799	775	619	593
30	1575	1592	1545	1404	1313

6. Sensitivity Analysis

In order to figure out the impact of the input variables (i.e., f_c , B, L, T, and f_y) on P_{exp} , the mutual information (MI) method was used to analyze the importance of each variable. The MI method is a filtering method used to capture arbitrary relationships (both linear and nonlinear) between each independent variable and the target object, and thus an estimated amount of mutual information between each independent variable and the target object can be obtained [96]. Furthermore, the estimated amount lies between [0, 1]; when it is 0 then the two variables are independent and when it is 1 then the two variables are perfectly correlated. In other words, when the estimated amount is closer to 1, it means the correlation between the two variables is stronger. Based on this, the results of the relevance between these five inputs and P_{exp} were shown in Figure 16. Intuitively, f_y and T showed a

significant correlation with P_{exp} , with the respective correlation indices of 0.457 and 0.432, followed by B and f_c , whose values of correlation indices with P_{exp} are 0.255 and 0.233, respectively. As for L, it showed an insignificant correlation with P_{exp} because of the low correlation index of 0.061.

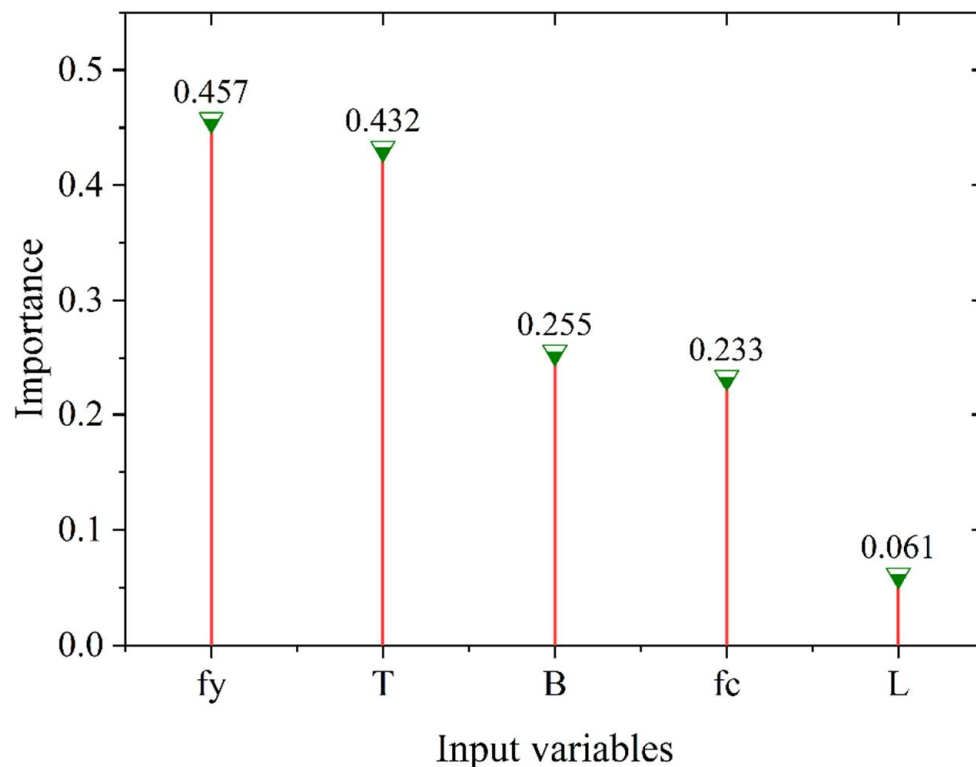


Figure 16. Importance of input variables.

7. Limitations and Future Investigations

Model generalization is one of the common limitations in concrete technology and civil engineering studies. In this study, we considered only square cases of the SCFST columns, and therefore, we used 149 data samples for modeling purposes. The proposed models are able to predict the bearing capacity of the SCFST columns if the input parameters on new data are within the range of our input parameters. Previous researchers pioneered the concept of combining theories and empirical formulas with ML/AI methods, which has been refined.

The civil engineering communities would benefit from more investigation into this topic since a pure ML/AI model is not appealing enough to be employed. The ability to include theories and empirical formulae into the data preparation stage for a specific issue would be of the utmost importance to civil engineers at all levels. It is vital to emphasize that civil engineers do not often have enough knowledge of computer science or ML/AL models. The well-known theories and formula in this field of study may be used to create a new database, which will result in improved model performance and prediction accuracy.

8. Conclusions

This research considered one of the most comprehensive databases of square SCFST columns and the bearing capacity of these columns were estimated using a series of analysis and computations. To accomplish this, the most critical parameters of the ICA-ANN and PSO-ANN models were created using a comprehensive modelling procedure. Then, their predictive ability for the bearing capacities of SCFST columns was evaluated using a variety of statistical evaluation indicators. In addition, the bearing capacities of SCFST columns

were also calculated using two well-known standards and a comparison was performed. The following findings have been made as a result of this investigation:

1. Both metaheuristic-based ANN approaches performed an acceptable performance in the prediction phase, as they were able to offer values for bearing capacity close to those measured in the laboratory.
2. This study's results indicated that the PSO-ANN model performed much better than the ICA-ANN model in both the model construction and evaluation processes. R^2 values of 0.936 and 0.873 for PSO-ANN and ICA-ANN models indicate that PSO is more powerful than the ICA method at determining the optimal weights and biases of ANN.
3. The comparison between measured bearing capacities together with those predicted by metaheuristic-based ANN models as well as different standards showed that both PSO-ANN and ICA-ANN models are more accurate compared to available standards. This confirmed that such intelligent techniques are needed to be used in order to obtain closer bearing capacities to the measured values.
4. Results of feature importance indicated that f_y and T , with significant correlations of 0.457 and 0.432 respectively, have the highest effects on the bearing capacity of SCFST columns. Therefore, a higher level of care regarding these parameters and their designs should be considered in the laboratory while tests are planned and conducted.

Author Contributions: Conceptualization, P.S., D.J.A. and M.M.S.S.; methodology, D.J.A.; software, P.S., B.H. and D.J.A.; formal analysis, D.J.A. and P.S.; resources, P.S. data curation, H.J., writing—original draft, D.J.A., P.S., M.M.S.S., B.H., D.V.U. and H.J.; writing—review and editing, D.J.A., P.S., M.M.S.S., B.H., D.V.U. and H.J.; Supervision, D.V.U. and H.J.; funding acquisition M.M.S.S. All authors have read and agreed to the published version of the manuscript.

Funding: The research is partially funded by the Ministry of Science and Higher Education of the Russian Federation under the strategic academic leadership program 'Priority 2030' (Agreement 075-15-2021-1333 dated 30 September 2021).

Acknowledgments: The first authors' great gratitude goes to Tongji University for its support in using the facilities of the university, financial aids, and its library access during this study.

Conflicts of Interest: The authors declare that they have no conflict of interest.

References

1. Pires, T.A.C.; Rodrigues, J.P.C.; Silva, J.J.R. Fire resistance of concrete filled circular hollow columns with restrained thermal elongation. *J. Constr. Steel Res.* **2012**, *77*, 82–94. [[CrossRef](#)]
2. De Lorenzis, L.; Stratford, T.J.; Hollaway, L.C. Structurally deficient civil engineering infrastructure: Concrete, metallic, masonry and timber structures. In *Strengthening and Rehabilitation of Civil Infrastructures Using Fibre-Reinforced Polymer (FRP) Composites*; Woodhead Publishing-Elsevier: Sawston, UK, 2008; pp. 1–44.
3. Shen, S.-L.; Wang, Z.-F.; Sun, W.-J.; Wang, L.-B.; Horpibulsuk, S. A field trial of horizontal jet grouting using the composite-pipe method in the soft deposits of Shanghai. *Tunn. Undergr. Sp. Technol.* **2013**, *35*, 142–151. [[CrossRef](#)]
4. Chitawadagi, M.V.; Narasimhan, M.C.; Kulkarni, S.M. Axial strength of circular concrete-filled steel tube columns—DOE approach. *J. Constr. Steel Res.* **2010**, *66*, 1248–1260. [[CrossRef](#)]
5. De Oliveira, W.L.A.; De Nardin, S.; de Cresce El, A.L.H.; El Debs, M.K. Influence of concrete strength and length/diameter on the axial capacity of CFT columns. *J. Constr. Steel Res.* **2009**, *65*, 2103–2110. [[CrossRef](#)]
6. Hunaiti, Y.M. Composite action of foamed and lightweight aggregate concrete. *J. Mater. Civ. Eng.* **1996**, *8*, 111–113. [[CrossRef](#)]
7. Giakoumelis, G.; Lam, D. Axial capacity of circular concrete-filled tube columns. *J. Constr. Steel Res.* **2004**, *60*, 1049–1068. [[CrossRef](#)]
8. Gupta, P.K.; Sarda, S.M.; Kumar, M.S. Experimental and computational study of concrete filled steel tubular columns under axial loads. *J. Constr. Steel Res.* **2007**, *63*, 182–193. [[CrossRef](#)]
9. Han, L.-H.; Li, W.; Bjorhovde, R. Developments and advanced applications of concrete-filled steel tubular (CFST) structures: Members. *J. Constr. Steel Res.* **2014**, *100*, 211–228. [[CrossRef](#)]
10. Zheng, Y.; Usami, T.; Ge, H. Ductility evaluation procedure for thin-walled steel structures. *J. Struct. Eng.* **2000**, *126*, 1312–1319. [[CrossRef](#)]
11. Liu, J.; Teng, Y.; Zhang, Y.; Wang, X.; Chen, Y.F. Axial stress-strain behavior of high-strength concrete confined by circular thin-walled steel tubes. *Constr. Build. Mater.* **2018**, *177*, 366–377. [[CrossRef](#)]

12. Sakino, K.; Nakahara, H.; Morino, S.; Nishiyama, I. Behavior of centrally loaded concrete-filled steel-tube short columns. *J. Struct. Eng.* **2004**, *130*, 180–188. [[CrossRef](#)]
13. Tao, Z.; Wang, Z.-B.; Yu, Q. Finite element modelling of concrete-filled steel stub columns under axial compression. *J. Constr. Steel Res.* **2013**, *89*, 121–131. [[CrossRef](#)]
14. Han, L.-H.; Liu, W.; Yang, Y.-F. Behaviour of concrete-filled steel tubular stub columns subjected to axially local compression. *J. Constr. Steel Res.* **2008**, *64*, 377–387. [[CrossRef](#)]
15. Skalomenos, K.A.; Hatzigeorgiou, G.D.; Beskos, D.E. Parameter identification of three hysteretic models for the simulation of the response of CFT columns to cyclic loading. *Eng. Struct.* **2014**, *61*, 44–60. [[CrossRef](#)]
16. Zhang, W.H.; Wang, R.; Zhao, H.; Lam, D.; Chen, P. Axial-load response of CFST stub columns with external stainless steel and recycled aggregate concrete: Testing, mechanism analysis and design. *Eng. Struct.* **2022**, *256*, 113968. [[CrossRef](#)]
17. Natalli, J.F.; Xavier, E.M.; Costa, L.C.B.; Rodrigues, B.H.; Sarmanho, A.M.C.; Peixoto, R.A.F. New methodology to analyze the steel–concrete bond in CFST filled with lightweight and conventional concrete. *Mater. Struct.* **2021**, *54*, 13. [[CrossRef](#)]
18. Chen, W.; Sarir, P.; Bui, X.-N.; Nguyen, H.; Tahir, M.M.; Armaghani, D.J. Neuro-genetic, neuro-imperialism and genetic programming models in predicting ultimate bearing capacity of pile. *Eng. Comput.* **2020**, *36*, 1101–1115. [[CrossRef](#)]
19. Parsajoo, M.; Armaghani, D.J.; Mohammed, A.S.; Khari, M.; Jahandari, S. Tensile strength prediction of rock material using non-destructive tests: A comparative intelligent study. *Transp. Geotech.* **2021**, *31*, 100652. [[CrossRef](#)]
20. Du, C.; Liu, X.; Liu, Y.; Tong, T. Prediction of the Interface Shear Strength between Ultra-High-Performance Concrete and Normal Concrete Using Artificial Neural Networks. *Materials* **2021**, *14*, 5707. [[CrossRef](#)]
21. Kovačević, M.; Lozančić, S.; Nyarko, E.K.; Hadzima-Nyarko, M. Modeling of compressive strength of self-compacting rubberized concrete using machine learning. *Materials* **2021**, *14*, 4346. [[CrossRef](#)]
22. Armaghani, D.J.; Harandzadeh, H.; Momeni, E.; Maizir, H.; Zhou, J. An optimized system of GMDH-ANFIS predictive model by ICA for estimating pile bearing capacity. *Artif. Intell. Rev.* **2021**, *55*, 2313–2350. [[CrossRef](#)]
23. Li, C.; Zhou, J.; Armaghani, D.J.; Li, X. Stability analysis of underground mine hard rock pillars via combination of finite difference methods, neural networks, and Monte Carlo simulation techniques. *Undergr. Sp.* **2021**, *6*, 379–395. [[CrossRef](#)]
24. Armaghani, D.J.; Mohamad, E.T.; Narayanasamy, M.S.; Narita, N.; Yagiz, S. Development of hybrid intelligent models for predicting TBM penetration rate in hard rock condition. *Tunn. Undergr. Sp. Technol.* **2017**, *63*, 29–43. [[CrossRef](#)]
25. Asteris, P.G.; Rizal, F.I.M.; Koopialipoor, M.; Roussis, P.C.; Ferentinou, M.; Armaghani, D.J.; Gordan, B. Slope Stability Classification under Seismic Conditions Using Several Tree-Based Intelligent Techniques. *Appl. Sci.* **2022**, *12*, 1753. [[CrossRef](#)]
26. Mahmood, W.; Mohammed, A.S.; Asteris, P.G.; Kurda, R.; Armaghani, D.J. Modeling Flexural and Compressive Strengths Behaviour of Cement-Grouted Sands Modified with Water Reducer Polymer. *Appl. Sci.* **2022**, *12*, 1016. [[CrossRef](#)]
27. Asteris, P.G.; Lourenço, P.B.; Roussis, P.C.; Adami, C.E.; Armaghani, D.J.; Cavaleri, L.; Chaliouris, C.E.; Hajihassani, M.; Lemonis, M.E.; Mohammed, A.S. Revealing the nature of metakaolin-based concrete materials using artificial intelligence techniques. *Constr. Build. Mater.* **2022**, *322*, 126500. [[CrossRef](#)]
28. Khajehzadeh, M.; Keawsawasvong, S.; Sarir, P.; Khailany, D.K. Seismic Analysis of Earth Slope Using a Novel Sequential Hybrid Optimization Algorithm. *Period. Polytech. Civ. Eng.* **2022**, *66*, 355–366. [[CrossRef](#)]
29. Jiang, H.; Mohammed, A.S.; Kazeroon, R.A.; Sarir, P. Use of the Gene-Expression Programming Equation and FEM for the High-Strength CFST Columns. *Appl. Sci.* **2021**, *11*, 10468. [[CrossRef](#)]
30. Zarringol, M.; Thai, H.-T.; Thai, S.; Patel, V. Application of ANN to the design of CFST columns. In *Proceedings of the Structures; Elsevier: Amsterdam, The Netherlands, 2020*; Volume 28, pp. 2203–2220.
31. Luat, N.-V.; Shin, J.; Lee, K. Hybrid BART-based models optimized by nature-inspired metaheuristics to predict ultimate axial capacity of CCFST columns. *Eng. Comput.* **2020**, *38*, 1421–1450. [[CrossRef](#)]
32. Liao, J.; Asteris, P.G.; Cavaleri, L.; Mohammed, A.S.; Lemonis, M.E.; Tsoukalas, M.Z.; Skentou, A.D.; Maraveas, C.; Koopialipoor, M.; Armaghani, D.J. Novel Fuzzy-Based Optimization Approaches for the Prediction of Ultimate Axial Load of Circular Concrete-Filled Steel Tubes. *Buildings* **2021**, *11*, 629. [[CrossRef](#)]
33. Vu, Q.-V.; Truong, V.-H.; Thai, H.-T. Machine learning-based prediction of CFST columns using gradient tree boosting algorithm. *Compos. Struct.* **2021**, *259*, 113505. [[CrossRef](#)]
34. Tran, V.-L.; Thai, D.-K.; Kim, S.-E. Application of ANN in predicting ACC of SCFST column. *Compos. Struct.* **2019**, *228*, 111332. [[CrossRef](#)]
35. Ren, Q.; Li, M.; Zhang, M.; Shen, Y.; Si, W. Prediction of ultimate axial capacity of square concrete-filled steel tubular short columns using a hybrid intelligent algorithm. *Appl. Sci.* **2019**, *9*, 2802. [[CrossRef](#)]
36. Le, T.-T. Practical machine learning-based prediction model for axial capacity of square CFST columns. *Mech. Adv. Mater. Struct.* **2020**, *29*, 1782–1797. [[CrossRef](#)]
37. Seghier, M.E.A.B.; Gao, X.-Z.; Jafari-Asl, J.; Thai, D.-K.; Ohadi, S.; Trung, N.-T. Modeling the nonlinear behavior of ACC for SCFST columns using experimental-data and a novel evolutionary-algorithm. In *Proceedings of the Structures; Elsevier: Amsterdam, The Netherlands, 2021*; Volume 30, pp. 692–709.
38. Mai, S.H.; Seghier, M.E.A.B.; Nguyen, P.L.; Jafari-Asl, J.; Thai, D.-K. A hybrid model for predicting the axial compression capacity of square concrete-filled steel tubular columns. *Eng. Comput.* **2022**, *38*, 1205–1222. [[CrossRef](#)]
39. Specht, D.F. A general regression neural network. *IEEE Trans. Neural Netw.* **1991**, *2*, 568–576. [[CrossRef](#)]

40. Al-Bared, M.A.M.; Mustafa, Z.; Armaghani, D.J.; Marto, A.; Yunus, N.Z.M.; Hasanipahan, M. Application of hybrid intelligent systems in predicting the unconfined compressive strength of clay material mixed with recycled additive. *Transp. Geotech.* **2021**, *30*, 100627. [[CrossRef](#)]
41. Paji, M.K.; Gordan, B.; Biklaryan, M.; Armaghani, D.J.; Zhou, J.; Jamshidi, M. Neuro-swarm and Neuro-imperialism Techniques to Investigate the Compressive Strength of Concrete Constructed by Freshwater and Magnetic Salty Water. *Measurement* **2021**, *182*, 109720. [[CrossRef](#)]
42. Simpson, P.K. *Artificial Neural Systems: Foundations, Paradigms, Applications, and Implementations*; Pergamon: Oxford, UK, 1990; ISBN 0080378943.
43. Jahed Armaghani, D.; Hajihassani, M.; Yazdani Bejarbaneh, B.; Marto, A.; Tonnizam Mohamad, E. Indirect measure of shale shear strength parameters by means of rock index tests through an optimized artificial neural network. *Meas. J. Int. Meas. Confed.* **2014**, *55*, 487–498. [[CrossRef](#)]
44. Khandelwal, M.; Marto, A.; Fatemi, S.A.; Ghoroghi, M.; Armaghani, D.J.; Singh, T.N.; Tabrizi, O. Implementing an ANN model optimized by genetic algorithm for estimating cohesion of limestone samples. *Eng. Comput.* **2017**, *34*, 307–317. [[CrossRef](#)]
45. Shao, Z.; Armaghani, D.J.; Bejarbaneh, B.Y.; Mu'azu, M.A.; Mohamad, E.T. Estimating the Friction Angle of Black Shale Core Specimens with Hybrid-ANN Approaches. *Measurement* **2019**, *145*, 744–755. [[CrossRef](#)]
46. Basheer, I.A.; Hajmeer, M. Artificial neural networks: Fundamentals, computing, design, and application. *J. Microbiol. Methods* **2000**, *43*, 3–31. [[CrossRef](#)]
47. Dreyfus, G. *Neural Networks: Methodology and Applications*; Springer: Berlin/Heidelberg, Germany, 2005; ISBN 3540288473.
48. Kennedy, J.; Eberhart, R.C. A discrete binary version of the particle swarm algorithm. In Proceedings of the 2009 IEEE international conference on Systems, Man and Cybernetics, Systems, Man, and Cybernetics, San Antonio, TX, USA, 11–14 October 2009; Computational Cybernetics and Simulation. Volume 5, pp. 4104–4108.
49. Brownlee, J. *Clever Algorithms: Nature-Inspired Programming Recipes*; Brownlee, J., Ed.; Lulu Press, Inc.: Morrisville, NC, USA, 2011; ISBN 1446785068.
50. Poli, R.; Kennedy, J.; Blackwell, T. Particle swarm optimization. *Swarm Intell.* **2007**, *1*, 33–57. [[CrossRef](#)]
51. Atashpaz-Gargari, E.; Lucas, C. Imperialist competitive algorithm: An algorithm for optimization inspired by imperialistic competition. In Proceedings of the IEEE Congress on Evolutionary Computation, CEC 2007, Singapore, 25–28 September 2007; pp. 4661–4667.
52. Mohamad, E.T.; Li, D.; Murlidhar, B.R.; Armaghani, D.J.; Kassim, K.A.; Komoo, I. The effects of ABC, ICA, and PSO optimization techniques on prediction of ripping production. *Eng. Comput.* **2019**, *36*, 1355–1370. [[CrossRef](#)]
53. Khandelwal, M.; Mahdiyar, A.; Armaghani, D.J.; Singh, T.N.; Fahimifar, A.; Faradonbeh, R.S. An expert system based on hybrid ICA-ANN technique to estimate macerals contents of Indian coals. *Environ. Earth Sci.* **2017**, *76*, 399. [[CrossRef](#)]
54. Armaghani, D.J.; Koopialipour, M.; Marto, A.; Yagiz, S. Application of several optimization techniques for estimating TBM advance rate in granitic rocks. *J. Rock Mech. Geotech. Eng.* **2019**, *11*, 779–789. [[CrossRef](#)]
55. Lee, Y.; Oh, S.-H.; Kim, M.W. The effect of initial weights on premature saturation in backpropagation learning. In Proceedings of the IJCNN-91-Seattle International Joint Conference on Neural Networks, Seattle, WA, USA, 8–14 July 1991; Volume 1, pp. 765–770.
56. Mohamad, E.T.; Faradonbeh, R.S.; Armaghani, D.J.; Monjezi, M.; Majid, M.Z.A. An optimized ANN model based on genetic algorithm for predicting ripping production. *Neural Comput. Appl.* **2017**, *28*, 393–406. [[CrossRef](#)]
57. Tran-Ngoc, H.; Khatir, S.; Ho-Khac, H.; De Roeck, G.; Bui-Tien, T.; Wahab, M.A. Efficient Artificial neural networks based on a hybrid metaheuristic optimization algorithm for damage detection in laminated composite structures. *Compos. Struct.* **2021**, *262*, 113339. [[CrossRef](#)]
58. Mohamad, E.T.; Armaghani, D.J.; Momeni, E.; Yazdavar, A.H.; Ebrahimi, M. Rock strength estimation: A PSO-based BP approach. *Neural Comput. Appl.* **2018**, *30*, 1635–1646. [[CrossRef](#)]
59. Mohammed, A.; Kurda, R.; Armaghani, D.J.; Hasanipahan, M. Prediction of compressive strength of concrete modified with fly ash: Applications of neuro-swarm and neuro-imperialism models. *Comput. Concr.* **2021**, *27*, 489–512.
60. Zeng, J.; Roy, B.; Kumar, D.; Mohammed, A.S.; Armaghani, D.J.; Zhou, J.; Mohamad, E.T. Proposing several hybrid PSO-extreme learning machine techniques to predict TBM performance. *Eng. Comput.* **2021**, 1–17. [[CrossRef](#)]
61. Mahdiyar, A.; Armaghani, D.J.; Marto, A.; Nilashi, M.; Ismail, S. Rock Tensile Strength Prediction Using Empirical and Soft Computing Approaches. *Bull. Eng. Geol. Environ.* **2019**, *78*, 4519–4531. [[CrossRef](#)]
62. Song, T.-Y.; Han, L.-H.; Yu, H.-X. Concrete filled steel tube stub columns under combined temperature and loading. *J. Constr. Steel Res.* **2010**, *66*, 369–384. [[CrossRef](#)]
63. Lachemi, M.; Hossain, K.M.A.; Lambros, V.B. Self-consolidating concrete filled steel tube columns? Design equations for confinement and axial strength. *Struct. Eng. Mech.* **2006**, *22*, 541–562. [[CrossRef](#)]
64. Li, N.; Wang, L.; Xi, Y.; Wang, H.; Guan, T.; Dong, F.; Sui, C.; Cui, W. The experimental research on axial compression performance of concrete-filled steel square tube strengthened by internal transverse stiffened bars. *Funct. Mater.* **2017**, *24*, 5–433. [[CrossRef](#)]
65. Xiang, X.; Cai, C.S.; Zhao, R.; Peng, H. Numerical analysis of recycled aggregate concrete-filled steel tube stub columns. *Adv. Struct. Eng.* **2016**, *19*, 717–729. [[CrossRef](#)]
66. Feng, P.; Cheng, S.; Bai, Y.; Ye, L. Mechanical behavior of concrete-filled square steel tube with FRP-confined concrete core subjected to axial compression. *Compos. Struct.* **2015**, *123*, 312–324. [[CrossRef](#)]

67. Chen, Z.; Ning, F.; Mo, L. Experimental study and mechanism analysis of concrete-filled square steel tubular columns reinforced inclined square stirrups under axial compression. *Front. Mater.* **2021**, *8*, 92. [[CrossRef](#)]
68. Reddy, G.S.R.; Bolla, M.; Patton, M.L.; Adak, D. Comparative study on structural behaviour of circular and square section-Concrete Filled Steel Tube (CFST) and Reinforced Cement Concrete (RCC) stub column. In *Proceedings of the Structures*; Elsevier: Amsterdam, The Netherlands, 2021; Volume 29, pp. 2067–2081.
69. Huang, Z.; Uy, B.; Li, D.; Wang, J. Behaviour and design of ultra-high-strength CFST members subjected to compression and bending. *J. Constr. Steel Res.* **2020**, *175*, 106351. [[CrossRef](#)]
70. Zhu, T.; Liang, H.; Lu, Y.; Li, W.; Zhang, H. Axial behaviour of slender concrete-filled steel tube square columns strengthened with square concrete-filled steel tube jackets. *Adv. Struct. Eng.* **2020**, *23*, 1074–1086. [[CrossRef](#)]
71. Phan, D.H.H.; Patel, V.I.; Liang, Q.Q.; Al Abadi, H.; Thai, H.-T. Simulation of uniaxially compressed square ultra-high-strength concrete-filled steel tubular slender beam-columns. *Eng. Struct.* **2021**, *232*, 111795. [[CrossRef](#)]
72. Tao, Z.; Han, L.-H.; Wang, D.-Y. Experimental behaviour of concrete-filled stiffened thin-walled steel tubular columns. *Thin-Walled Struct.* **2007**, *45*, 517–527. [[CrossRef](#)]
73. Zhu, M.; Liu, J.; Wang, Q.; Feng, X. Experimental research on square steel tubular columns filled with steel-reinforced self-consolidating high-strength concrete under axial load. *Eng. Struct.* **2010**, *32*, 2278–2286. [[CrossRef](#)]
74. Chen, B.; Liu, X.; Li, S. Performance investigation of square concrete-filled steel tube columns. *J. Wuhan Univ. Technol. Sci. Ed.* **2011**, *26*, 730–736. [[CrossRef](#)]
75. Yang, Y.F.; Han, L.H. Concrete filled steel tube (CFST) columns subjected to concentrically partial compression. *Thin-Walled Struct.* **2012**, *50*, 147–156. [[CrossRef](#)]
76. Lee, S.-H.; Choi, Y.-H.; Kim, Y.-H.; Choi, S.-M. Structural performance of welded built-up square CFST stub columns. *Thin-walled Struct.* **2012**, *52*, 12–20. [[CrossRef](#)]
77. Prabhu, G.G.; Sundarraja, M.C. Behaviour of concrete filled steel tubular (CFST) short columns externally reinforced using CFRP strips composite. *Constr. Build. Mater.* **2013**, *47*, 1362–1371. [[CrossRef](#)]
78. Aslani, F.; Uy, B.; Tao, Z.; Mashiri, F. Behaviour and design of composite columns incorporating compact high-strength steel plates. *J. Constr. Steel Res.* **2015**, *107*, 94–110. [[CrossRef](#)]
79. Ding, F.; Liu, J.; Liu, X.; Yu, Z.; Li, D. Mechanical behavior of circular and square concrete filled steel tube stub columns under local compression. *Thin-Walled Struct.* **2015**, *94*, 155–166. [[CrossRef](#)]
80. Sarir, P.; Chen, J.; Asteris, P.G.; Armaghani, D.J.; Tahir, M.M. Developing GEP tree-based, neuro-swarm, and whale optimization models for evaluation of bearing capacity of concrete-filled steel tube columns. *Eng. Comput.* **2019**, *37*, 1–19. [[CrossRef](#)]
81. Liou, S.W.; Wang, C.M.; Huang, Y.F. Integrative discovery of multifaceted sequence patterns by frame-relayed search and hybrid PSO-ANN. *J. Univers. Comput. Sci.* **2009**, *15*, 742–764.
82. Hecht-Nielsen, R. Kolmogorov's mapping neural network existence theorem. In *Proceedings of the International Conference on Neural Networks*, San Diego, CA, USA, 21–24 June 1987; IEEE Press: New York, NY, USA, 1987; Volume 3, pp. 11–13.
83. Mohamad, E.T.; Armaghani, D.J.; Noorani, S.A.; Saad, R.; Alvi, S.V.; Abad, N.K. Prediction of flyrock in boulder blasting using artificial neural network. *Electron. J. Geotech. Eng.* **2012**, *17*, 2585–2595.
84. Saghatforoush, A.; Monjezi, M.; Faradonbeh, R.S.; Armaghani, D.J. Combination of neural network and ant colony optimization algorithms for prediction and optimization of flyrock and back-break induced by blasting. *Eng. Comput.* **2016**, *32*, 255–266. [[CrossRef](#)]
85. Ebrahimi, E.; Monjezi, M.; Khalesi, M.R.; Armaghani, D.J. Prediction and optimization of back-break and rock fragmentation using an artificial neural network and a bee colony algorithm. *Bull. Eng. Geol. Environ.* **2016**, *75*, 27–36. [[CrossRef](#)]
86. Alavi Nezhad Khalil Abad, S.V.; Yilmaz, M.; Jahed Armaghani, D.; Tugrul, A. Prediction of the durability of limestone aggregates using computational techniques. *Neural Comput. Appl.* **2016**, *29*, 423–433. [[CrossRef](#)]
87. Jahed Armaghani, D.; Mohd Amin, M.F.; Yagiz, S.; Faradonbeh, R.S.; Abdullah, R.A. Prediction of the uniaxial compressive strength of sandstone using various modeling techniques. *Int. J. Rock Mech. Min. Sci.* **2016**, *85*, 174–186. [[CrossRef](#)]
88. Armaghani, D.J.; Asteris, P.G. A comparative study of ANN and ANFIS models for the prediction of cement-based mortar materials compressive strength. *Neural Comput. Appl.* **2020**, *33*, 4501–4532. [[CrossRef](#)]
89. Momeni, E.; Yarivand, A.; Bagher Dowlathshahi, M.; Jahed Armaghani, D. An Efficient Optimal Neural Network Based on Gravitational Search Algorithm in Predicting the Deformation of Geogrid-Reinforced Soil Structures. *Transp. Geotech.* **2020**, *26*, 100446. [[CrossRef](#)]
90. Zhou, J.; Asteris, P.G.; Armaghani, D.J.; Pham, B.T. Prediction of ground vibration induced by blasting operations through the use of the Bayesian Network and random forest models. *Soil Dyn. Earthq. Eng.* **2020**, *139*, 106390. [[CrossRef](#)]
91. Zhou, J.; Qiu, Y.; Zhu, S.; Armaghani, D.J.; Khandelwal, M.; Mohamad, E.T. Estimation of the TBM advance rate under hard rock conditions using XGBoost and Bayesian optimization. *Undergr. Sp.* **2020**, *6*, 506–515. [[CrossRef](#)]
92. Hasanipanah, M.; Monjezi, M.; Shahnezari, A.; Armaghani, D.J.; Farazmand, A. Feasibility of indirect determination of blast induced ground vibration based on support vector machine. *Measurement* **2015**, *75*, 289–297. [[CrossRef](#)]
93. Lu, S.; Koopialipoor, M.; Asteris, P.G.; Bahri, M.; Armaghani, D.J. A Novel Feature Selection Approach Based on Tree Models for Evaluating the Punching Shear Capacity of Steel Fiber-Reinforced Concrete Flat Slabs. *Materials* **2020**, *13*, 3902. [[CrossRef](#)] [[PubMed](#)]

94. Koopialipoor, M.; Jahed Armaghani, D.; Hedayat, A.; Marto, A.; Gordan, B. Applying various hybrid intelligent systems to evaluate and predict slope stability under static and dynamic conditions. *Soft Comput.* **2019**, *23*, 5913–5929. [[CrossRef](#)]
95. Code, P. *Eurocode 4: Design of Structures for Earthquake Resistance-Part 1: General Rules, Seismic Actions and Rules for Buildings*; European Committee for Standardization: Brussels, Belgium, 2005.
96. Verron, S.; Tiplica, T.; Kobi, A. Fault Detection and Identification with a New Feature Selection Based on Mutual Information. *J. Process Control* **2008**, *18*, 479–490. [[CrossRef](#)]